Title
Development of a Simplified Multizone Infiltration Model

Author
Feustel, H.E.

Publication Date
1985-11-01

Lawrence Berkeley Laboratory

UNIVERSITY OF CALIFORNIA

APPLIED SCIENCE DIVISION

Published in the Proceedings of the 6th AIC Conference, Het Meerdal, Netherlands, September 16-21, 1985

DEVELOPMENT OF A SIMPLIFIED MULTIZONE INFILTRATION MODEL

H.E. Feustel

November 1985

APPLIED SCIENCE DIVISION

Prepared for the U.S. Department of Energy under Contract DE-AC03-76SF00098

LBL-19095
EEB-EPB-85-14

Published in *Proceedings*, 6th AIC Conference, Het Meerdal, Netherlands, September 16-21, 1985.

DEVELOPMENT OF A SIMPLIFIED MULTIZONE INFILTRATION MODEL

Helmut E. Feustel
Applied Science Division
Lawrence Berkeley Laboratory
University of California
Berkeley, CA 94720, USA

November 1985

This work was supported by the Assistant Secretary for Conservation and Renewable Energy, Office of Building Energy Research and Development, Building Systems Division of the U.S. Department of Energy under Contract No. DE-AC03-76SF00098.

Abstract

Several infiltration models treat the complexity of air flows in multizone buildings, but most of them are written as research tools and are not generally available or user-friendly. Professional engineers and architects are in need of a simplified multizone infiltration model. This paper describes the first step in Lawrence Berkeley Laboratory's development of a multizone infiltration model for calculating the air-flow distribution of a building without using any iteration procedure. To simplify the calculation procedure, buildings are classified into different categories, based on their ratios of permeabilities. These lumped parameters describing the air permeability distribution of a building are used to calculate its overall infiltration/exfiltration rate. The simplified multizone model described is illustrated by a sample calculation.

Keywords: Multizone Infiltration, Air-Flow Modeling, Lumped Parameters.

1. Table of Symbols

c_k	pressure coefficient for surface element k [-]
$\overline{c}_{lee}$	average pressure coefficient on the leeward side [-]
$\overline{c}_{luv}$	average pressure coefficient on the windward side [-]
g	acceleration of gravity $[m/s^2]$
j	number of considered story [-]
k	number of stories [-]
m	air mass flow [kg/h]
n	exponent of the pressure difference [-]
p_0	atmospheric pressure [Pa]
p_{dyn}	dynamic pressure in the undisturbed flow [Pa]
p_i	inside pressure [Pa]
p_k	pressure at surface element k [Pa]
p_o	outside pressure [Pa]
Δp_{stack}	pressure difference due to stack [Pa]
Δp_{tot}	pressure difference due to stack and wind action [Pa]
Δp_{wind}	pressure difference due to wind [Pa]
v	wind velocity [m/s]
x, y, z	coordinates [m]
z_0	reference height for wind velocity measurements [m],
D	air permeability of the building component $[m^3/h\ Pa^n]$
$D_{lee,envelope}$	air permeability of the leeward side of the building envelope $[m^3/h\ Pa^n]$
D_r	resultant permeability at reference conditions $[m^3/h\ Pa^n]$
D_{res}	resultant permeability $[m^3/h\ Pa^n]$
D_{shaft}	air permeability from the story to the shaft $[m^3/h\ Pa^n]$
$D_{total,envelope}$	air permeability of the total building envelope $[m^3/h\ Pa^n]$
H	height of the building [m]
NPL	neutral pressure level [m]
Q	air flow through a building component $[m^3/h]$
Q_r	air flow at reference conditions $[m^3/h]$
Q_{tot}	superposition of flows $[m^3/h]$
Q_{wind}	air flow due to wind $[m^3/h]$
Q_{stack}	air flow due to temperature differences $[m^3/h]$
α	exponent [-]; value depends on terrain roughness[3,4]
ϕ	wind direction $[^\circ]$, usually 10 m above ground
ρ_o	density of the outside air $[kg/m^3]$
ρ_i	density of the inside air $[kg/m^3]$

2. Introduction

Numerous computer programs have been developed to calculate infiltration-related energy loss in buildings. To treat the true complexity of air flows in a multizone building requires extensive information about flow characteristics and pressure distribution; accordingly, simplified models have been developed. Most of these models, including the one developed at Lawrence Berkeley Laboratory (LBL), simulate infiltration associated with single-cell structures. A high percentage of existing buildings, however, have floor plans that characterize them more accurately as multizone structures, which cannot be treated by single-cell models. Although multizone models exist, most are either not generally available or are written as research tools [1]. Professional engineers and architects are in need of a simplified multizone infiltration model capable of providing the same accuracy as the existing single-zone models. In this paper the first steps in developing a simplified infiltration model for multizone buildings are explained and preliminary results are shown.

3. Modeling Infiltration in Multizone Buildings

3.1 Outline

Air flow through the building envelope is a combination of viscous and turbulent flow. Two different mechanisms are responsible for natural air flow in buildings -- wind pressure and thermal buoyancy forces. The distribution of openings in the building shell and the inner flow-paths influence the patterns of air flow.

In terms of air flow, a building can be regarded as a complicated, interlaced grid system of flow paths [2]. In this grid system the joints are the rooms of the buildings and the connections between the joints simulate the flow paths, which include flow resistances caused by open or closed doors and windows and/or air leakage through the walls. The grid points outside the building represent the boundary conditions for the pressure. Differences in air density, caused by differences between outside and inside air temperatures, result in additional pressures in the vertical direction, again influencing the building's air flow.

In buildings with mechanical ventilation systems, the duct system can be treated as another interior flow path and the fan as another source of pressure differences; i.e., the fan lifts the pressure level between two joints according to the characteristic curve of the fan. The HVAC components, such as heating and cooling coils, constitute additional sources of pressure loss.

Because of the nonlinear dependency of the volume flow on the pressure difference, the pressure distribution has usually been calculated by using a method of iterations. To describe buildings with complicated floor plans and to solve the set of nonlinear equations requires large computer storage capacity.

3.2 Physical Fundamentals of the Pressure Distribution

Wind flows produce a velocity and pressure field around the building. Compared to the static pressure associated with an undisturbed wind-velocity pattern, the pressure field around a building is generally characterized by regions of overpressure on the windward side and underpressure on the facades parallel to the air stream and on the leeward side of the building. The pressure distribution is usually described by dimensionless pressure coefficients; that is, the ratio of the surface pressure and the dynamic pressure in the undisturbed flow pattern:

$$c_k(x, y, z, \phi) = \frac{p_k(x, y, z) - p_0(z)}{p_{dyn}(z)} \tag{1}$$

with

$$p_{dyn}(z) = \frac{1}{2} \rho_o \; v^2(z) \tag{2}$$

The vertical profile for the wind speed in the atmospheric boundary layer depends primarily on the roughness of the surface surrounding the building. The wind speed increases with increasing height above ground. The wind velocity profile can be calculated either by a logarithmic equation or by a power law expression [3,4]. The latter is usually used by engineers and building scientists.

$$\frac{v(z)}{v(z_0)} = \left\{ \frac{z}{z_0} \right\}^{\alpha} \tag{3}$$

Both mentioned equations describing the wind velocity profile assume that the wind flow is isothermal and horizontal. Furthermore, it is assumed that the wind flow will not change its direction as a result of differences in the terrain surface.

As noted, temperature differences between the outside and inside air create air density differences that cause pressure gradients. The stack-effect pressure gradient depends only on temperature differences and the vertical dimension of the structure [5,6,7]. The theoretical value of the pressure difference is dependent on the gradient and the distance of the neutral pressure level (NPL), which is defined as the height on the building facade where, under calm conditions, no pressure difference exists between inside and outside. The permeability distribution of the envelope determines the location of the NPL. The stack effect (or thermal buoyancy) can be calculated by the equation

$$\frac{d(p_i - p_o)}{dz} = g\ (\rho_o - \rho_i) \tag{4}$$

and, after integration,

$$(p_i - p_o)_{stack} = g\ (\rho_o - \rho_i)\,(z - NPL) \tag{5}$$

3.3 Building Classification

For purposes of modeling infiltration, buildings are classified as one of the following:

(a) row house (terrace house)
(b) detached house
(c) story-type house
(d) shaft-type house

These four basic categories (see Fig. 1) reflect different permeability distributions of the building's envelope (influence of the wind effect) and different vertical flow resistances inside the building (influence of the stack effect) [8,9].

The distinction between the four categories can be expressed by two permeability ratios. Krischer and Beck [8] used the following parameter to describe the envelope permeability ratio (*epr*) of the whole building for a given house type in categories a or b:

$$epr = \frac{D_{lee,envelope}}{D_{total,envelope}} \tag{6}$$

Based on Krischer and Beck's investigation, the *epr* of row houses can be described by the average permeability ratio of the leeward side to the overall permeability of the building envelope of *epr* = 0.5, whereas the corresponding value for a detached house rises to *epr* = 0.75.

In the latest issue of the German standard, DIN 4701 [10], another parameter, internal vertical permeability, was introduced to further differentiate construction types in categories c and d. For further considerations, it is useful to also introduce the ratio of the permeabilities from one floor to another and the overall permeability of the building envelope. Eq. 7 describes the building vertical permeability ratio (*vpr*) for a given construction type for the whole building.

$$vpr = \frac{D_{shaft}}{D_{total,envelope} + D_{shaft}} \tag{7}$$

With regard to the thermal pressure distribution, two extremes exist: story-type buildings with no permeability between floors ($vpr = 0$) and shaft-type buildings with no air-flow resistance between the different stories ($vpr = 1$).

Parameters similar to those explained above were used in DIN 4701 to calculate the *maximum* air flow for the whole building so that the *maximum* possible heat loss due to infiltration could be calculated for each zone of a building at the design condition for the heating system.

To describe the air-flow distribution for the different zones at the story level, we defined two more lumped parameters [11,12]: the outside permeability ratio (*opr*) of the zone (which describes the influence on cross ventilation of the zone, cross ventilation being the portion of the air flow that exfiltrates out of the same zone where it infiltrates -- see Eq. 8), and the inside permeability ratio (*ipr*) of the zone (which describes the stack influence of the zone -- see Eq. 9).

$$opr = \frac{D_{zone,lee,outside\ envelope}}{D_{zone,outside\ envelope}} \tag{8}$$

$$ipr = \frac{D_{zone,shaft}}{D_{zone,outside\ envelope} + D_{zone,shaft}} \tag{9}$$

In a previous study, the use of a detailed multizone infiltration model showed a strong relationship between the two latter ratios and the flow distribution in buildings [11]. With increasing values for *opr* and decreasing values for *ipr*, the zones become more wind-dominated. Consequently, increasing *ipr*'s in combination with decreasing *opr*'s show the opposite effect.

Based on simulations using a detailed model [2,9,11], the ratios described in Eq. 6 - 9 can be used as parameters in a simplified model. In other words, the infiltration can be calculated as:

$$Q_{wind} = f\,(D_{lee}, D_{shaft}, epr, vpr, opr, ipr, v(z_0), \alpha, n, z, \phi, H) \tag{10}$$

and

$$Q_{stack} = f\,(D_{lee}, D_{shaft}, epr, vpr, opr, ipr, t_i, t_o, n, z, H, NPL) \tag{11}$$

3.4 Infiltration and Exfiltration

3.4.1 General Considerations

The following illustrations of the physical fundamentals of air-flow distribution in buildings are based on four assumptions:

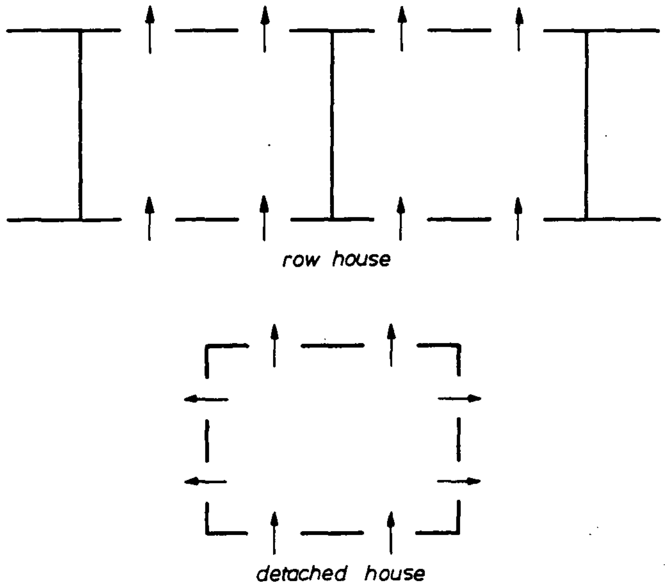

Fig. 1a: Subdivision on the Building Type according to the Permeability Ratio of the Building Envelope.

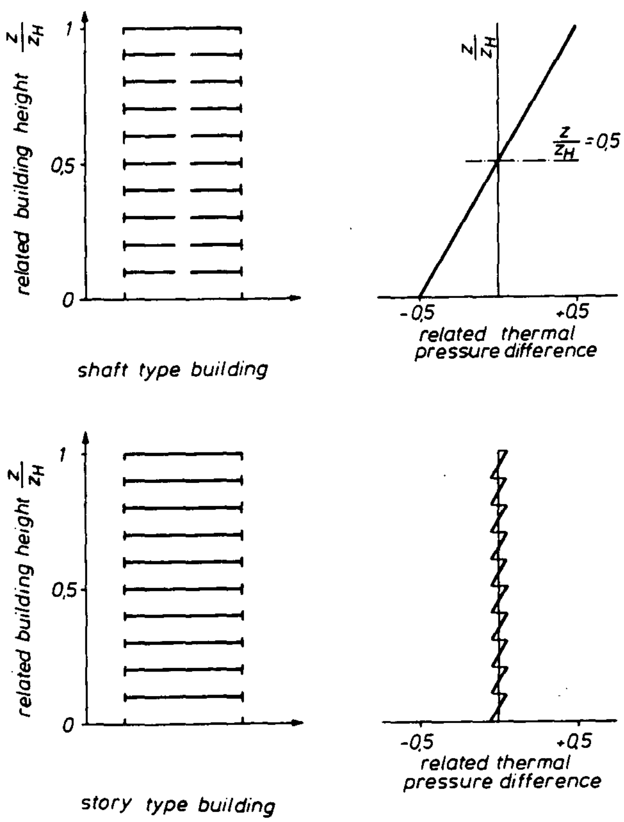

Fig. 1b: Thermal Pressure Difference as a Function of the Type of Construction and $t_i > t_o$

1) The building has a simplified floor plan; all infiltrated air of a story passes a reference point;
2) The wind flows perpendicular to the windward facade of the building;
3) The vertical wind velocity profile can be expressed by a power-law expression;
4) No changes in the direction of wind flow occur as a result of other structures in the neighborhood of the building.

The only way of eliminating assumptions 2 to 4 is to use surface pressure measurements either on full-scale buildings or on models in the wind tunnel.

3.4.2 Physical Fundamentals

3.4.2.1 Air Flow through Openings

The permeability of a building's envelope is mainly determined by the number of cracks, windows, doors, and gaps between building components. Besides these observable visual leaks, there is background leakage caused by the porosity of building material, and cracks in these materials. Leakage measurements of building components and wall sections were reported as early as the second and third decade of this century (e.g. reviewed by Brinkmann [13]), and more recent articles, dealing with air flows through cracks were published by Kronvall [14] and McGrath [15]. The pressure drop along the crack length is expressed in terms of friction and resistance whereas the air flow through building components is usually described by the empirical power-law equation:

$$Q = D\ (p_1 - p_2)^n \qquad (12)$$

The value of the air permeability and the exponent can be measured by the fan pressurization technique (DC) [16] or the AC pressurization technique [17]. The value of the exponent n can be expected to be between its physical limits of $n = 1.0$ for fully developed laminar flow and $n = 0.5$ for fully developed turbulent flow. Because of the intake and outlet losses, which are proportional to the square of the mean flow velocity, the exponent cannot become 1.0. On the other hand, for short flow length the friction becomes negligible compared to the intake and outlet losses. In that case the flow resistance can be treated like a local loss coefficient similar to the ones used to calculate duct losses ($n = 0.5$). A comparison of air leakage in 196 houses, by measure of the blower door technique (DC), showed, for the whole house, a mean value 0.66 for the exponent [18], which is in good agreement with the measured flow characteristic, n, of building components [19,20].

Usually the effective air permeability for a building is a combination of air permeabilities arranged in series, or parallel, or both. Parallel permeabilities can be easily added, but for a series arrangement permeability can be calculated as follows:

$$Q = D_{res} \left\{ (p_1 - p_2) + (p_2 - p_3) + \cdots + (p_{k-1} - p_k) \right\}^n \tag{13}$$

$$Q = D_1 (p_1 - p_2)^n = D_2 (p_2 - p_3)^n = D_{k-1} (p_{k-1} - p_k)^n \tag{14}$$

$$D_{res} = \left\{ D_1^{-1/n} + D_2^{-1/n} + \cdots + D_{k-1}^{-1/n} \right\}^{-n} \tag{15}$$

The use of these equations assumes that all permeabilities have the same flow characteristics, which means having the same exponent, n. Fig. 2 shows the resultant air permeability for two resistances in a series arrangement with an exponenent n = 2/3.

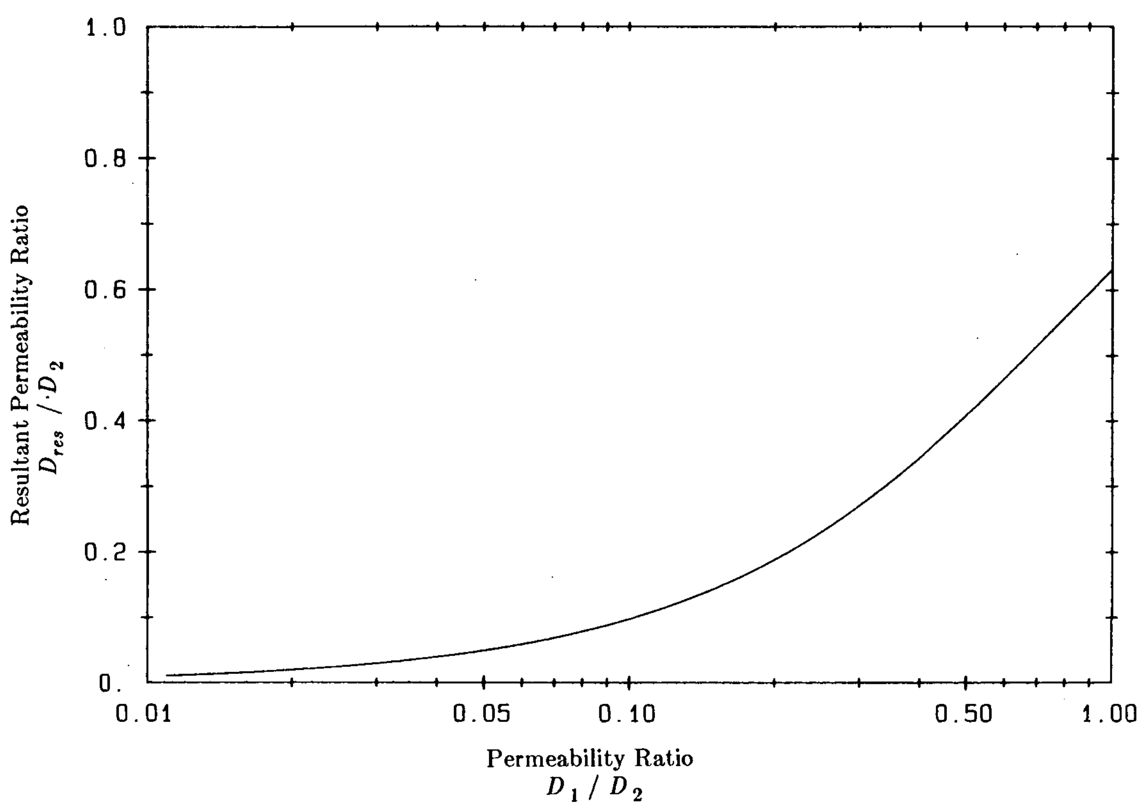

Fig. 2: Resultant Air Permeability for Series Arrangement

3.4.2.2 Superposition of Flows

Air-flows caused by the separate mechanisms of wind and thermal buoyancy are not additive because the flow rates are not linearly proportional to the pressure differences. Therefore, to superpose the flows, the pressures have to be added. The superposed volume rate can generally be calculated by:

$$Q_{tot} = D\ (\Delta p_{tot})^n \tag{16}$$

$$Q_{tot} \approx D\ (\Delta p_{wind} + \Delta p_{stack})^n \tag{17}$$

$$Q_{tot} \approx (Q_{wind}{}^{1/n} + Q_{stack}{}^{1/n})^n \tag{18}$$

Because each mechanism might force the air to flow in a different direction, the superposition of the flows for each facade and each story is given as:

$$Q_{tot} = sign\ |\,(sign\ |\,Q_{wind}\,|^{1/n} + sign\ |\,Q_{stack}\,|^{1/n})\,|^{\,n} \tag{19}$$

According to Eq. 19 both driving forces for natural ventilation can be calculated separately and superposed to obtain the total natural ventilation.

3.4.2.3 Air Flow due to Stack

The difference in thermal pressure for a given temperature difference under calm conditions is a linear function of the distance of the height above ground from the neutral pressure level (NPL -- see. Eq. 5). Therefore, the volume rate driven by thermal buoyancy only is:

$$Q_{stack}(z) = D_{res}(z)\ [\Delta p_{stack}(z)]^n \tag{20}$$

$$\Delta p_{stack} = (p_i - p_o)^n_{stack} \tag{21}$$

$D_{res}(z)$ is the resultant permeability calculated for the arrangement of permeabilities in series or parallel between the place where the stack pressure occurs (elevator shaft, stair well, etc.) and the outside. For an apartment building, these permeabilities might be the elevator door, doors to individual apartments, doors inside the apartments, and the openings of the facades. In addition to the pressure gradient in shafts and vertical ducts there is the same bouyancy effect at each individual story of the building. Because of the limited height of the story and the relatively small distances of the different openings from the local NPL of the story, these pressure differences are negligible compared to those forced by wind and by the chimney effect of internal shafts.

3.4.2.4 Air Flow due to Wind

To calculate the pressure differences caused by wind, one has to know the outside pressure field as well as the internal pressure at a reference point. The reference point has to be located at a place where all infiltrated air flow from a given story passes. If such a reference point cannot be found for a building, the following simplifications are not applicable. The internal pressure is a function of the permeability distribution of the building's envelope and of the internal flow resistances. From the continuity equation one can derive the air flow for each story:

$$\rho_o \; D_{luv}(z) \, [\Delta p_{wind,luv}(z,\phi,T,epr,vpr)]^n = \rho_i \; D_{shaft}(z) \, [p_i(z,epr,vpr) - p_{shaft}]^n$$

$$+ \rho_i \; D_{lee}(z) \left\{ \Delta p_i(z,epr,vpr) - [p_{dyn}(z) \, \overline{c}_{lee}(z,\phi)] \right\}^n \quad (22)$$

In this case the permeability D_{luv} is the resultant permeability of all flow path between the facade of the windward side and the reference point. This has to be handled respectively for the leeward side. For story-type buildings this set of equations can be solved independently for each story using Eq. 23:

$$\Delta p_i(z,epr,vpr) = p_i(z,epr,vpr=0) - p_0(z) = \quad (23)$$

$$\frac{\left\{ [\rho_o \; D_{luv}(z)]^{1/n} \; p_{dyn}(z) \, \overline{c}_{luv}(z,\phi) \right\} + \left\{ [\rho_i \; D_{lee}(z)]^{1/n} \; p_{dyn}(z) \, \overline{c}_{lee}(z,\phi) \right\}}{[\rho_o \; D_{luv}(z)]^{1/n} + [\rho_i \; D_{lee}(z)]^{1/n}}$$

For all other building types ($vpr \neq 0.0$) this set of equations (Eq. 22) has to be solved by using a method of iterations.

To simplify the infiltration model, a method for determining the internal pressure of a building has to be developed. The inside pressure distribution due to wind will become uniform with an increasing permeability from the stories to the shaft. The pressure difference responsible for the wind-driven air flow can be calculated by:

$$\Delta p_{wind,luv}(z,\phi,T,epr,vpr) =$$

$$\frac{\rho_o}{2}\left\{v(z_0)\left[\frac{z}{z_0}\right]^{\alpha}\right\}^2 \overline{c}_{luv}(z,\phi) - \Delta p_i(z,epr,vpr) \qquad (24)$$

This pressure difference is mainly a function of the building's height above ground and the building type. The volume rate driven by wind action only can be calculated by:

$$Q_{wind}(z,\phi,epr,vpr) = D_{luv}(z)\,[\Delta p_{wind,luv}(z,\phi,epr,vpr)]^n \qquad (25)$$

3.4.3 Simplifications of Air Flow Calculations

3.4.3.1 Thermal Buoyancy

The calculation of air flow caused by the stack effect, as shown in Eq. 20, is very simple. For those who use pocket calculators, the algorithm can be simplified even further. In the following three equations we define a dimensionless volume ratio $q(z)$ that describes the air-flow caused by stack effect for a given temperature difference at a given distance from NPL divided by the air-flow at reference conditions:

$$q(z) = \frac{Q(z)}{Q_r} \qquad (26)$$

$$q(z) = \frac{D(z)\,(p_i - p_o)^n}{D_r\,(p_i - p_o)_r^n} \qquad (27)$$

If the permeability is evenly distributed over the building height and the temperature difference is equal to the one used to calculate the air-flow at the reference point, the volume ratio can be expressed as

$$q(z) = \frac{(z - NPL)^n}{(z_r - NPL)^n} \qquad (28)$$

which is plotted in Fig. 3 for n = 2/3. Therefore, after calculating Q_r, the whole calculation of stack-related infiltration could be done using Fig. 3.

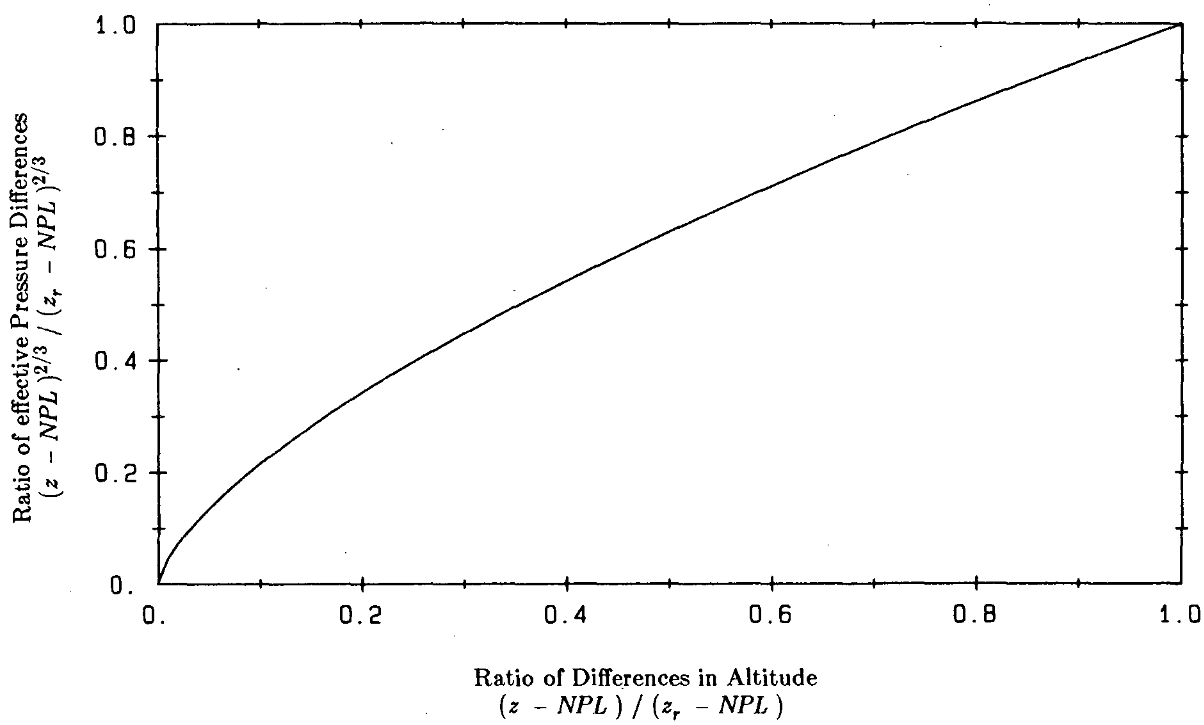

Fig. 3: Ratio of effective Pressure Difference vs. Ratio of Differences in Altitude from NPL

3.4.3.2 Wind Action

Besides the determination of the permeability distribution and the pressure field around the building, the most difficult aspect of calculating wind-driven infiltration is the determination of the inside pressure of the house. Because the air-flow through the shaft due to wind action and thermal buoyancy causes no significant friction losses in the shaft, it can be assumed to have no pressure gradient inside the shaft itself. Furthermore, a uniform distribution of the shaft leakage over the height of the shaft could be expected. This, in conjunction with Eq. 29, can be used to calculate the pressure of the shaft as a first approximation, which is shown in Eq. 30:

$$0 = \sum_{j=1}^{k} \left\{ p_i(j) - p_{shaft} \right\}^n \approx \sum_{j=1}^{k} \left\{ p_i(j) - p_{shaft} \right\} \qquad (29)$$

$$p_{shaft} = \frac{1}{k} \sum_{j=1}^{k} p_i(j) \tag{30}$$

For this calculation the inside pressures of story-type buildings might be used. A further simplification for calculating the pressure of the shaft would be to use the average of the inside pressures for the top and bottom story.

$$p_{shaft} = 1/2 \left\{ p_i(j=1, epr, vpr=0) + p_i(j=k, epr, vpr=0) \right\} \tag{31}$$

This calculation gives slightly different values for the shaft pressure than does the calculation presented in Eq. 30. It uses the inside pressure from Eq. 23 for buildings with the envelope permeability ratio *epr* for detached houses or row houses as input. For that calculation story-type buildings with a central corridor and a symmetrical floor plan, certain surface pressure coefficients of $c_{luv} = 1.0$ for the windward side and $c_{lee} = -0.3$ for the leeward side and perpendicular air flow [8] are assumed.

Using Eq. 22 the inside pressure for a story-type building can be calculated as:

$$p_i(z, epr, vpr=0) - p_0(z) = X(epr, vpr=0)\ p_{dyn}(z) \tag{32}$$

with

$$X(epr=0.75, vpr=0) = -0.09$$
$$X(epr=0.50, vpr=0) = 0.35$$

A comparison of different infiltration models [2] revealed the importance of the air flow through the shaft, even when no stack effect is present. The high pressures at the top of the building cause a downstream of infiltrated air in the shaft. This air is released into the lower levels of the building. This is an extremely significant effect for the flow distribution in houses having small *epr*-values. The following empirical equation gives the approximate value for the inside pressures as a function of the building's height above ground and the building type.

$$p_i(z, epr, 0<vpr<1) = p_{shaft}$$

$$+ \frac{\left\{ p_i(z=H, epr, vpr=0) - p_{shaft} \right\}}{H/2} (1 - vpr^n)(z - H/2) \quad (33)$$

With these assumptions the necessary data for the inside pressure distribution for the calculation of wind driven air-flow using Eq. 25 are determined.

3.5 Example of Application of Simplified Model

3.5.1 General

The use and accuracy of this simplified model for calculating overall infiltration and exfiltration in a multi-story building having a simple floor plan, (see Fig. 4) is shown in this section. Results will be compared for accuracy with data from a detailed multizone model [2], that uses the same kind of input for the permeabilities and weather conditions. These results are plotted in Fig. 5 and Fig. 6.

3.5.2 Boundary Conditions

The boundary conditions for both, the simplified and detailed mathematical models are given in Table 1.

Table 1: Input data for multizone model

outdoor temperature	0 °C
inside temperature	20 °C
height of stories	3 m
number of stories	18
wind speed at reference height	4 m/s
reference height for wind speed measurement	10 m
exponent for vertical wind profile	1/3
exponent for pressure differences	2/3
surface pressure coefficients at windward side	1.
surface pressure coefficient at leeward side	-0.3
air permeability of building components (per Fig. 4)	$m^3/h\ Pa^n$

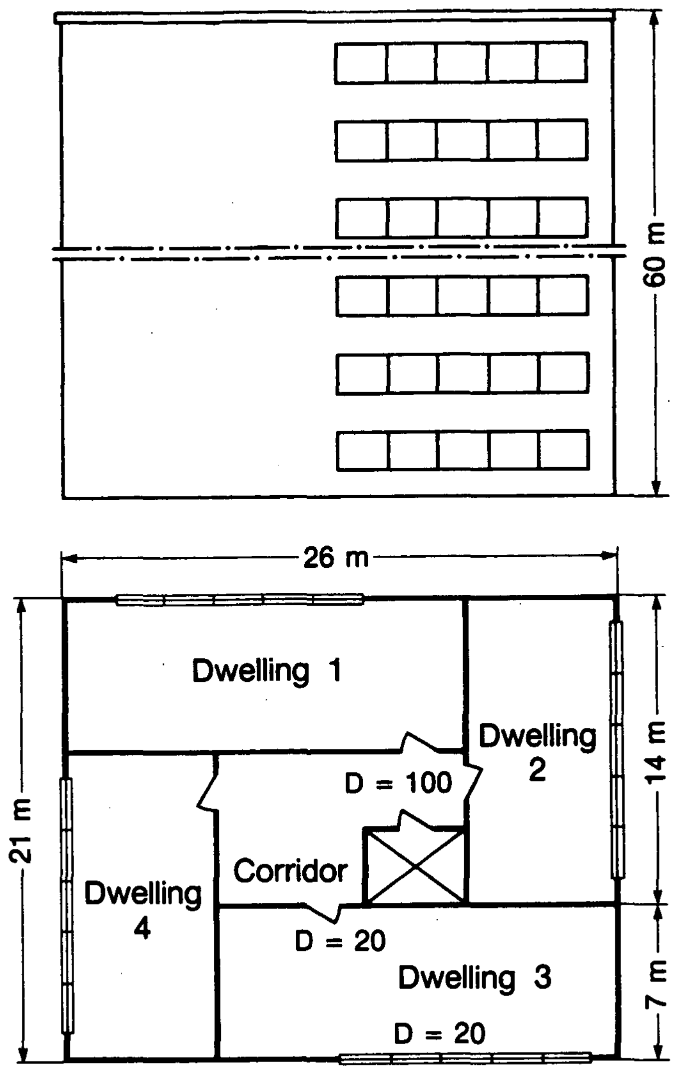

Fig. 4: Simplified Floor Plan and Elevation

3.5.3 Results and Discussion

Comparison shows that the air mass flows due to natural ventilation are reasonably identical whether calculated with the detailed model or the simplified equations given in 3.4.3. The differences in results obtained with both models on the air flows on the windward side are very small at the bottom of the building and increase with the height above ground. The error of the overall infiltration rate for the whole windward side of the building is less than 5%, the difference between both models reaches almost 20% on the top floor.

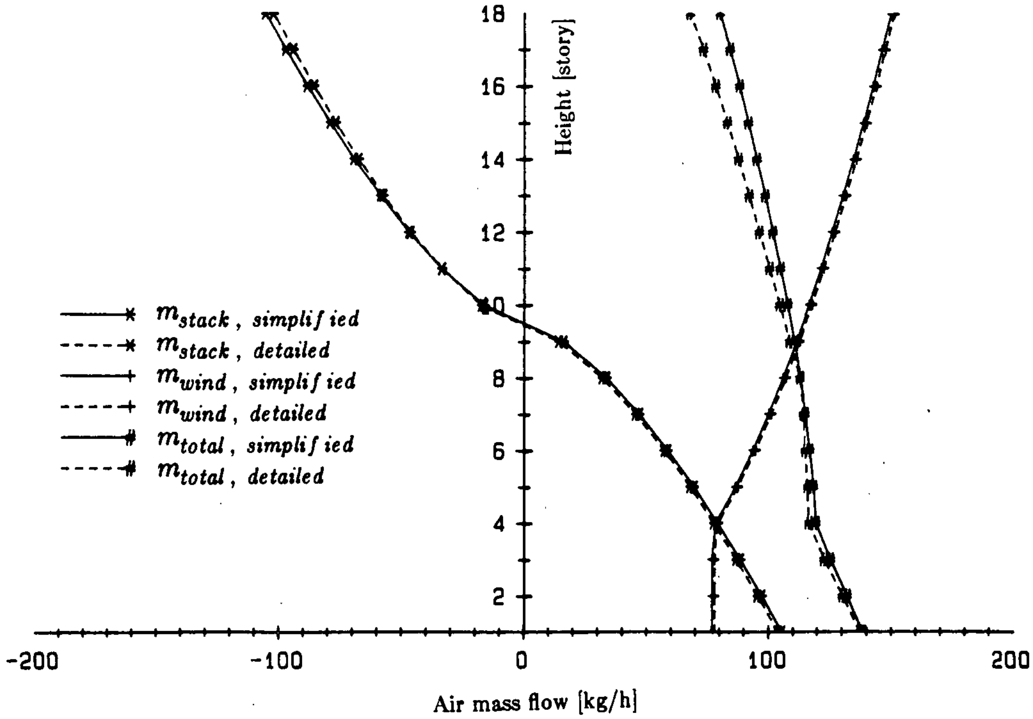

Fig. 5: Air Mass Flow for the Windward Side

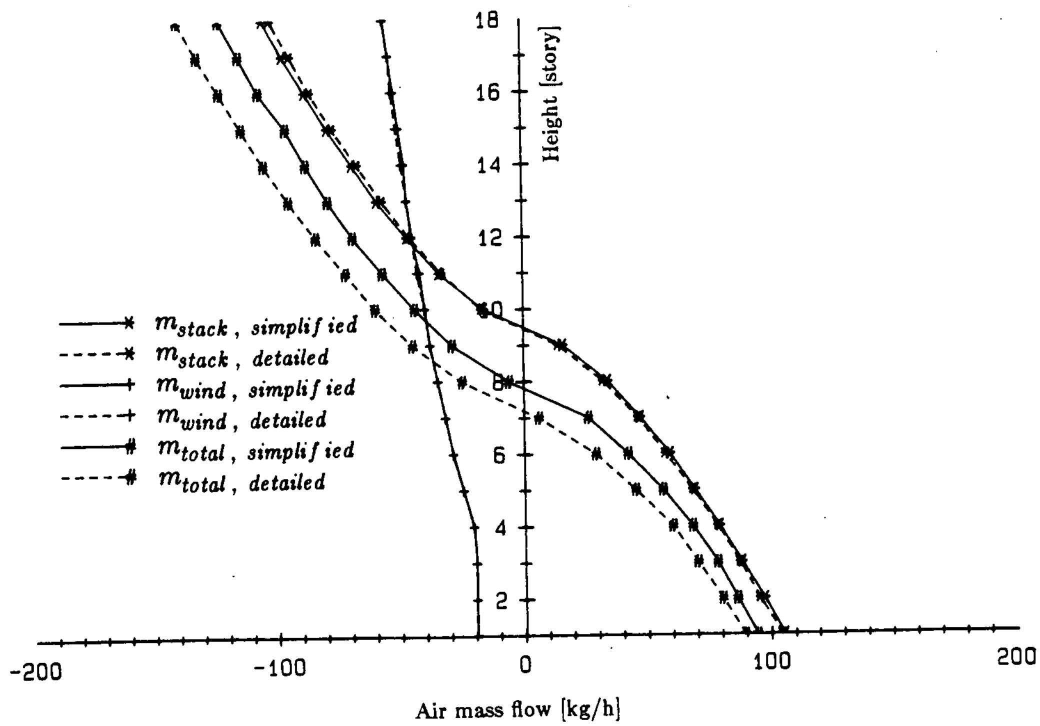

Fig. 6: Air Mass Flow for the Leeward Side

(for each of the three zones)

Because of the smaller pressure difference between the envelope surface at the leeward side and the reference point inside the building, the simple algorithm used to calculate the inside pressure distribution produces significant differences between the exfiltration air flows, particularly in cases where the separate flows caused by wind action and thermal buoyancy are converse in their direction. The greatest relative differences (400%) are seen in the area of the NPL of the leeward side. The overall exfiltration is still in the range of ± 20% of the reference value given by the detailed program.

Nevertheless, this example shows that the simplified equations presented here can be used to calculate infiltration rates even for high-rise buildings. The advantage of this algorithm is that it does not require iteration procedures.

3.5.4 Conclusions

In most infiltration models two important parameters --the pressure field around the building and the permeability distribution of the external and internal building components--are usually estimated only roughly. For evaluation and application of models both these parameters must be determined. With the growing proliferation of wind tunnel studies, one might soon be able to predict the pressure field around a building: but the need remains for a multizone pressurization method capable of yielding necessary information about a building's air permeability distribution. Until both of these input parameters can be determined, all multizone infiltration models will be handicapped.

This research is critical to solving the problems of infiltration simulation for multizone buildings, and should receive international attention.

We at LBL intend to focus our studies on the air flow distribution between different zones using *opr* and *ipr* as guiding principles. One goal is to be able to calculate the air flow even when the wind direction is not perpendicular to the windward side of the building.

4. Summary

In describing the simplified multizone infiltration model developed at LBL, the physical fundamentals involved in the pressure distribution caused by wind action and the stack effect as well as air flow through a building's openings are discussed. Buildings are classified into different categories based on their air permeability distribution, an important step in reducing the input data and limiting the different cases that might occur. When extreme cases for vertical permeability distribution are used as a base, extremes of air-flow distribution can be studied. All other structures are in between these extremes.

The example shows the importance of the compensatory air flow between stories when only wind action is present (compare Q_{wind} in Fig. 5 and Fig. 6). Models that restrict the air flow due to wind action to the story under consideration only, miss an important part of the air-flow distribution in a building.

It has been shown that, by adding the pressures, the air flow due to wind action and the air flow due to stack effect can be calculated separately and superposed later. This calculation allows the air infiltration and exfiltration for buildings with simple floor plans to be calculated without using an iteration method.

5. Acknowledgements

We gratefully acknowledge the assistance we received during the course of this work from the members of the Energy Performance of Buildings Group at LBL. The manuscript was kindly reviewed by M. Sherman, R. Szydlowski, D. Grimsrud and R. Kuelpmann.

This work was supported by the Assistant Secretary for Conservation and Renewable Energy, Office of Building Energy Research and Development, Building Systems Division of the U.S. Department of Energy under Contract No. DE-AC03-76SF00098.

6. References

[1] Feustel, H.E. and Kendon, V.M.:
"Infiltration Models for Multicellular Structures - A Literature Survey"
Lawrence Berkeley Laboratory, LBL #17588, 1985.

[2] Feustel, H.E.:
"Beitrag zur theoretischen Beschreibung der Druck- und Luftmassen-stromverteilung in natuerlich und maschinell geluefteten Gebaeuden"
Fortschritts-Bericht der VDI-Zeitschriften, Reihe 6, Nr. 151, VDI-Verlags GmbH, Duesseldorf, (1984).

[3] Davenport, A.G.:
"A Rationale for the Determination of Basic Design Wind Velocities"
ASCE *Proceedings* 86 (1960), pp. 36-68.

[4] Zuranzki, J.:
"Windbelastung von Bauwerken und Konstruktionen"
Verlagsgesellschaft Rudolf Mueller, Koeln-Braunsfels, (1969).

[5] Tamura, G.T. and Wilson, A.G.:
"Pressure Difference Caused by Chimney Effect in Three High-Rise Buildings"
ASHRAE Transactions, 73 (1967), Part II, pp. II.1.1-II.1.10.

[6] Tamura, G.T. and Wilson, A.G.:
"Building Pressures Caused by Chimney Action and Mechanical Ventilation"
ASHRAE Transactions, 73 (1967), Part II, pp. II.2.1.-II.2.12.

[7] Esdorn, H.:
"Luftdurchlaessigkeit der Fenster und Druckverteilung im Gebaeude"
In: Das Hochhaus der BASF "Planung, Ausfuehrung, Erfahrungen",
J. Hoffmann, Stuttgart, (1958).

[8] Krischer, O. and Beck, H.:
"Die Durchlueftung von Raeumen durch Windangriff und der Waermebedarf fuer die Lueftung"
VDI-Berichte, Vol. 18, 1957, 29-59.

[9] Zuercher, Ch. and Feustel, H.E.:
"Air Infiltration in High-Rise Buildings"
Proceedings of the 4th AIC Conference, Elm, Switzerland, (1983).

[10] Deutsches Institut fuer Normung. DIN 4701:
"Regeln fuer die Berechnung des Waermebedarfs von Gebaeuden"
Beuth Vertrieb Berlin, (1983).

[11] Feustel, H.E. and Lenz, Th.P.:
"Patterns of Infiltration in Multifamily Buildings"
Lawrence Berkeley Laboratory Report, LBL-17584, (1984).

[12] Feustel, H.E.:
"Multizone Infiltration Studies at Lawrence Berkeley Laboratory"
Proceedings, CLIMA 2000, Volume 6, Building Envelope Improvement, (1985).

[13] Brinkmann, W.:
"Zur Bestimmung des Lueftungswaermebedarfs hoher Gebaeude"
Doctoral Dissertation, Technische Universitaet Berlin, (1980).

[14] Kronvall, J.:
"Air Flow in Building Components"
Doctoral Dissertation, Lund Institute of Technology, (1980).

[15] McGrath, P.T.:
"The Prediction of Infiltration through Building Components; The Assembly of a Device to Measure Air Infiltration through Components with suggested Method of Producing Data Which Could Be used to form the Basis of a Prediction Model"
Dissertation, University of Manchester, (1982).

[16] ASTM Standard E 779 - 81
"Measuring Air Leakage by the Fan Pressurization Method"
ASTM Committee E-6 on Performance of Building Constructions, Philadelphia, (1981).

[17] Grimsrud, D.T.; Sherman, M.H. and Sonderegger, R.C.:
"Air Leakage in a Building at Low Pressures Using an Alternating Pressure Source"
Kongressbericht XXI. Intern. Kongress fuer Technische Gebaeudeausruestung, Teil 1, (1980), p. 124-127.

[18] Sherman, M.H.; Wilson, D.J. and Kiel, D.E.:
"Variability in Residential Air Leakage"
Proceedings, Symposium on Measured Air Leakage Performance of Buildings, ASTM, Philadelphia, (1984).

[19] Raisch, E.:
"Die Waerme- und Luftdurchlaessigkeit von Fenstern verschiedener Konstruktion"
GI Gesundheitsingenieur 45 (1922), p. 99-105.

[20] Reiher, H.; Fraass, K. and Settele, E.:
"Ueber die Frage der Luft- und Waermedurchlaessigkeit von Fenstern"
1. Teilbericht, Waermewirtschaftliche Nachrichten 6 (1932/33), pp. 42-59.

This report was done with support from the Department of Energy. Any conclusions or opinions expressed in this report represent solely those of the author(s) and not necessarily those of The Regents of the University of California, the Lawrence Berkeley Laboratory or the Department of Energy.

Reference to a company or product name does not imply approval or recommendation of the product by the University of California or the U.S. Department of Energy to the exclusion of others that may be suitable.

LAWRENCE BERKELEY LABORATORY
TECHNICAL INFORMATION DEPARTMENT
UNIVERSITY OF CALIFORNIA
BERKELEY, CALIFORNIA 94720